Review Paper

Sol-Gel Prepared NiO Thin Films for Electrochromic Applications

Romana Cerc Korošec and Peter Bukovec

Faculty of Chemistry and Chemical Techology, University of Ljubljana, Aškerčeva 5, SI-1000 Ljubljana, Slovenia
e-mail: romana.cerc-korosec@fkkt.uni-lj.si

Received 19-04-2006

Abstract

An electrochromic material changes its optical properties in the visible part of the spectrum under a certain applied potential. The change is reversible and the material returns to its original state under the opposite electric field. Recently, electrochromism has been applied in electrochromic devices, where in a battery-like assembly the throughput of solar light is controlled by the voltage and is usually termed a smart window. In the first part of this article a brief theoretical introduction to electrochromism and the functioning of smart windows is given. Since in the last decade nickel oxide has been extensively studied as an ion-storage material in electrochromic devices, some properties of nickel oxide are explained in the following part. The electrochromic response (reversibility during potential switching and the degree of coloration) of a nickel oxide thin film, used in a electrochromic device, strongly depends on the degree of heat treatment. Thermal analysis of thin films can give valuable information about a suitable temperature and the duration of heat-treatment when thin films are prepared by chemical methods of deposition. Since thermal analysis of thin films deposited on a substrate is not a common analytical technique, basic strategies are also summarized in the article. After this theoretical introduction, the application of TG analysis to optimisation of the electrochromic response of sol-gel prepared Ni oxide thin films is presented. The electrochromic properties of thin films, thermally treated to different degrees, were tested using spectroelectrochemical methods. Additional techniques (IR, TEM, AFM and EXAFS) were indispensable in following structural and morphological changes during the heat treatment.

Keywords: electrochromism, NiO thin films, thermal analysis, TG, sol-gel, optimisation

Contents

1. Electrochromism, electrochromic materials (ECMs) and electrochromic devices (ECDs) 136
2. lectrochromic nickel oxide thin films and the proposed coloration mechanism 138
3. Thermal analysis of thin films 139
4. Sol-gel prepared Ni oxide thin films from $NiSO_4$ precursor 140
5. Sol-gel prepared Ni oxide thin films from $Ni(CH_3COO)_2$ precursor 143
6. Conclusion 145
7. References 146

1. Electrochromism, electrochromic materials (ECMs) and electrochromic devices (ECDs)

By definition an electrochromic material is able to reversibly and persistently change its optical properties under an applied electric field.[1] Electrochromic materials came to public attention around 30 years ago after the report on the electrochromism of tungsten oxide by Deb.[2] Up to now, several different applications of electrochromic devices were developed, but for some of them – for *information displays*, for instance - commercialization has not taken place. Development was more successful in the case of e*lectrochromic automatically dimming rear-view mirrors*, which are now generally available for cars and trucks[3] and for *smart*

windows. Smart windows allow dynamic throughput control of light and solar energy,[4] and can be used as efficient solar protection against overheating during the time when a room is unoccupied and the device is switched to a coloured state. When the room is in use, smart windows in their bleached or intermediate darkened state assure adequate levels of illumination and optical contact with the environment outside the building. The energy saving implied in a smart window is the same as the electrical energy generated by a solar cell module of the same size placed in the same position.[5] Recently, some full-scale electrochromic smart windows are undergoing practical testing in buildings.[6] ECMs and devices have been reviewed several times in the past, and the literature up to 1993 is covered in detail in the monograph by Monk et al[7] and Granqvist[1]. Device-related work up to 2002 has been more recently reviewed.[8]

The various types of electrochromic substances may be divided into two general classes: transition metal oxides and organic materials. Within the inorganic substances there are two different types of coloration processes. Cathodically colouring transition metal oxides have reduced coloured states, while anodically colouring materials are those with an oxidized coloured state.

An important parameter distinguishing between electrochromic materials is the wavelength-dependant coloration efficiency (*CE*), expressed in cm^2/C and given by the expression:[4]

$$CE(\lambda) = \frac{\Delta OD(\lambda)}{\Delta Q} = \frac{\log(T_b / T_c)}{\Delta Q} \qquad (1)$$

where $\Delta\, OD(\lambda)$ is the change in optical density, T_b (λ) transmittance in the bleached and T_c (λ) transmittance in the coloured state. ΔQ corresponds to the inserted/extracted charge as a function per unit area. A large value of *CE* means that a small amount of electric charge is required for the colour change process. Table 1 summarizes some inorganic electrochromic oxides with large *CE* values.

Table 1. Summary of some most important inorganic electrochromic oxides.[1,9,10]

Oxide	POL	Colour	Coloration efficieny (*CE*) / $cm^2\,C^{-1}$
Co oxides	an	brown, black	from -11 to -25
IrO_2	an	blue, black	from -11 to -33
MoO_3	cat	blue	> 30
Nb_2O_3	cat	blue, brown	from 6 to 34
Ni oxides	an	brown, black	-36
RhO_2	an	green, black	similar as for IrO_2
V_2O_5	cat-an	green, blue, black	from 10 to 35
WO_3	cat	blue	from 30 to 60*

POL: polarization, an – anodic, cat – cathodic
**CE* greater then 100 $cm^2\,C^{-1}$ is reported during H^+ intercalation

The basic layout of an ECD consists of five layers (Figure 1).[1] On a transparent conducting electrode (1st layer), usually In_2O_3:Sn (ITO) or less costly SnO_2:F, an active electrochromic layer is deposited in the form of a thin film (2nd layer). An ion-conducting electrolytic laminate (3rd layer) connects the optically active material with an ion-storage material (4th layer), which is deposited on a second transparent conductive electrode (5th layer). An applied voltage (usually around 1 V), with appropriate polarity, drives the charge into the electrochromic material causing a change of absorption in the visible range of the spectrum.

Biographical Sketches

Romana Cerc Korošec *received her PhD in Chemistry in 2001 at University of Ljubljana for her work on Thermal, electrochromic and structural properties nickel oxide thin layers. She is particularly interested in thermal analysis of thin films, and has developed very applicable approach for TG and DSC measuring. Since 1996, she is the Assistant for Inorganic Chemistry at the Faculty of Chemistry and Chemical Technology, University of Ljubljana. She is currently interested in sol-gel chemistry of metal oxides and in thermal analysis of inorganic and polymeric materials.*

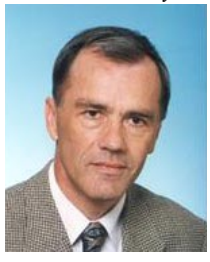

Peter Bukovec *was born in Ljubljana, Slovenia in 1946 and received his PhD in Chemistry in 1972 from University of Ljubljana. In 1973 he obtained the position of Assistant Professor and in 1984 the position of Professor of Inorganic Chemistry at the Faculty of Natural Sciences and Technology, University of Ljubljana. In 1980-81 he spent an Alexander von Humboldt post-doctoral year with R.Hoppe at Institute for Inorganic and Analytical Chemistry, Justus-Liebig University, Giessen, FRG. His current research interests include sol-gel chemistry of inorganic materials and the application of inorganic/organic hybrid materials.*

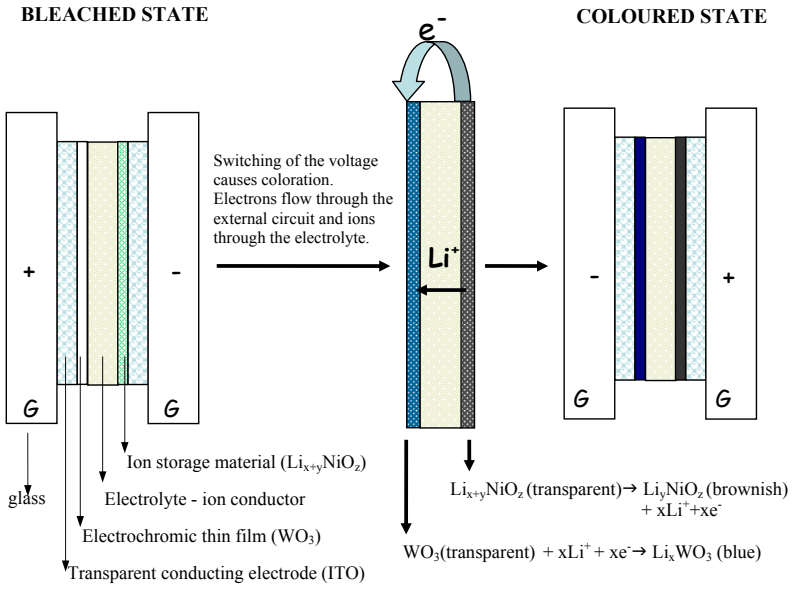

Figure 1. Construction of a basic ECD (WO_3/electrolyte/$Li_{x+y}NiO_z$) and reactions on coloration.

The most extensively studied electrochromic material is WO_3 owing to its large CE value (Table 1). Because of this attractive property it is most frequently used in device assemblies as the EC layer, usually called the working electrode. WO_3 belongs to the class of cathodic ECMs and reversibly switches from transparent (W^{6+}) to blue colour (W^{5+}) upon lithium ion or proton insertion. In combination with WO_3, the ion storage material (counter electrode) must be an anodic ECM. An optically neutral ECM (e.g. vanadium doped CeO_2) does not change its colour during ion insertion/extraction, so the colour change happens only on account of WO_3. On the other hand, the counter electrode can also be optically active, for instance Ni oxide. Upon oxidation, the colour changes from transparent (Ni^{2+}) to brownish (Ni^{3+}) at the same time as the WO_3 layer, yielding a grey coloured device in the coloured state. The term complementary ECD refers to simultaneous change in both the electrochromic and ion-storage layers. To assure the long-term stability and reversibility of the bleaching/colouring process, the amount of charge inserted at one side must match the amount of charge extracted at the other.[4] The time needed to colour the device should be as small as possible, preferably a few seconds. In Figure 1 the functioning of a complementary device during the colouring process is presented. Since Ni oxide is among the less understood electrode materials, a prelithiated NiO film, prepared by sputtering,[11] is taken as the ion-storage material for simplicity.

As reported recently, for a WO_3/NiO ECD, the transmittance change between coloured and bleached state is more than 65%.[5]

2. Electrochromic nickel oxide thin films and the proposed coloration mechanism

The interest in nickel oxide thin films is growing fast due to their importance in many applications in science and technology. Besides acting an EC material, it can also be used as a functional layer material for gas sensors.[12] Stoichiometric NiO is an insulator with a resistivity of the order of $10^{13}\ \Omega \cdot$ cm at room temperature.[13] Its resistivity can be lowered by an increase of Ni^{3+} ions resulting from addition of monovalent ions such as lithium, by the appearance of nickel vacancies, or by the presence of interstitial oxygen in the NiO crystallites.[14] The greater oxygen content originates from hydration of surface nickel atoms.[15]

Numerous studies have been performed in order to elucidate the electrochemical mechanism which takes place during the coloration/bleaching process.[16-18] The most recent study[19] reported that in the activation period an increase in capacity occurs, corresponding to chemical transformation $NiO + H_2O \rightarrow Ni(OH)_2$. Structural changes from NaCl type (bunsenite NiO) to layered $Ni(OH)_2$ occur upon amorphisation on the grain boundaries. In the steady state the reversible colour change from transparent to brownish involves the classical reaction $Ni(OH)_2 + OH^- \rightarrow NiOOH + H_2O + e^-$. NiO grains act as a reservoir of the electrochemically active hydroxide layer.[19] Several papers have reported that reversible electrochemical oxidation of Ni-atoms located at the NiO/electrolyte interface is responsible for a strong electrochromic effect[20-22], or that the electrochromic performance of nickel oxide depends on the size of the nanocrystallites.[23,24] Already in 1988

Estrada[25] observed that the optical properties of a thin film, consisting of grains about 7 nm in diameter, are stable for at least 5000 cycles, whereas for a 17 nm grain size a significant degradation was observed already after 50 cycles. The decrease in electrochromic properties after prolonged cycling is associated with dissolution of the NiOOH phase structure.[26] Recent investigations regarding a nickel oxide counter electrode include deposition of a thin protective layer on NiO when it is assembled together with WO_3.[5] WO_3 is stable in an acidic environment, but it dissolves in basic electrolytes. On the other hand, Ni oxide is stable in a basic environment, but unstable in acidic ones. A possible solution is to add a protective layer on top of the NiO film.[27]

Electrochromic nickel oxide thin films have been prepared by various physical (sputtering,[20] pulsed layer deposition,[26] electron-beam evaporation[15]) and chemical methods (atomic layer epitaxy,[28] sol-gel,[29] spray pyrolysis,[30] anodic deposition[31]). The films obtained differ in stoichiometry, structure, degree of crystallinity, crystallite size, etc. As a consequence, their electrochromic properties and colour efficiencies vary over a wide range. During or after the deposition process, the films have to be thermally treated in order to improve adhesion to substrate and to ensure their structural stability during cycling in an alkaline electrolyte. Regardless of the preparative technique, the degree of thermal treatment is the key factor which influences the magnitude of the optical modulation and stability of the film during the cycling process. Too high a processing temperature significantly lowers the electrochromic effect,[32] and the layer could even become inactive.[33] On the other hand, in thermally untreated films optical modulation decreases soon after the beginning of cycling.[29]

For chemically prepared thin films, thermal analysis of the films, together with complementary techniques (IR, EXAFS, TEM) gives valuable information. With the techniques mentioned we can follow thermal decomposition of the system, find out at which temperatures nickel oxide starts to form and when it is complete, determine crystallite size during decomposition and the residual species remaining in the thin film sample. Since thermal decomposition of thin films occurs at lower temperatures with regard to the corresponding xerogels,[29,34] it is important that measurements are performed on the films themselves. An explanation of the stoichiometric or structural properties of thin films using TG and DSC curves of the xerogels leads to a wrong interpretation.

3. Thermal analysis of thin films

Thermal analysis of thin films is a demanding procedure and direct measurements of thin films are still not very common.[35] This is the reason why in reported studies of the properties of chemically prepared NiO thin film thermal analysis is either made on the corresponding xerogels[30,36,37] or the investigated films are thermally treated at 200, 250 or 300 °C without performing TG analysis even for the xerogels.[21,38] The sensitivity of balances in TG instruments is in the order of 1 μg so that detection of the thermal decomposition of thin films is possible.[39] However, the amount of sample available is very small, typically below 1 mg, so that the mass change during a TG experiment is in the range of buoyancy and aerodynamic effects. In DSC measurements the evolved or absorbed heat diffuses into the substrate and consequently the measured enthalpies are very small.[40] The basic strategies for overcoming the above-mentioned difficulties were published in the 1990-ies in three review papers.[39-41]

In some cases thermal analysis of thin films can be performed in the usual manner:

- If the thin film exists as a free-standing (self-supporting) film, for instance thin metal films (Al foil), fast quenched amorphous alloys or thin films of polymers; the sample for TA need only be cut into small pieces or powdered and placed in the crucible (summarized examples are collected in [41]),
- If the thin film is deposited on a powdered substrate (TiO_2 on mica); a large active area of the substrate ensures enough sample for classical analysis[42],
- If the thickness of the thin film exceeds 1 μm; the thin film can be mechanically removed from the substrate.[43]

When the film is very thin (< 100 nm), it is difficult to get enough sample for analysis by scraping. But there are some methods for separating a thin film from the substrate.[44-47] The results obtained for deposited thin film samples and the corresponding xerogels can differ considerably due to differences in sample size, structure and microstructure.[41,48] Figure 2 summarizes suggestions collected in the mentioned review articles on how to perform thermal analysis measurements for thin film samples, deposited on a planar substrate.

If during a TG experiment a ferromagnetic metal or alloy is formed or consumed, the signal can be enhanced with the help of a strong external magnet. This method is called thermomagnetometry. The sensitivity in a strong field is such that one can nearly follow the oxidation of an atomic monolayer.[40] The principle is similar to that applied in the temperature calibration of TG apparatus.[56]

Emanation thermal analysis (ETA) is another sensitive method that has been used to characterize thin films prepared by sol-gel or chemical vapour deposition (CVD) methods. The solid is previously implanted with a radioactive gas or has it incorporated during its synthesis. During heating, the release of radioactive gas atoms from the solid sample is measured. When

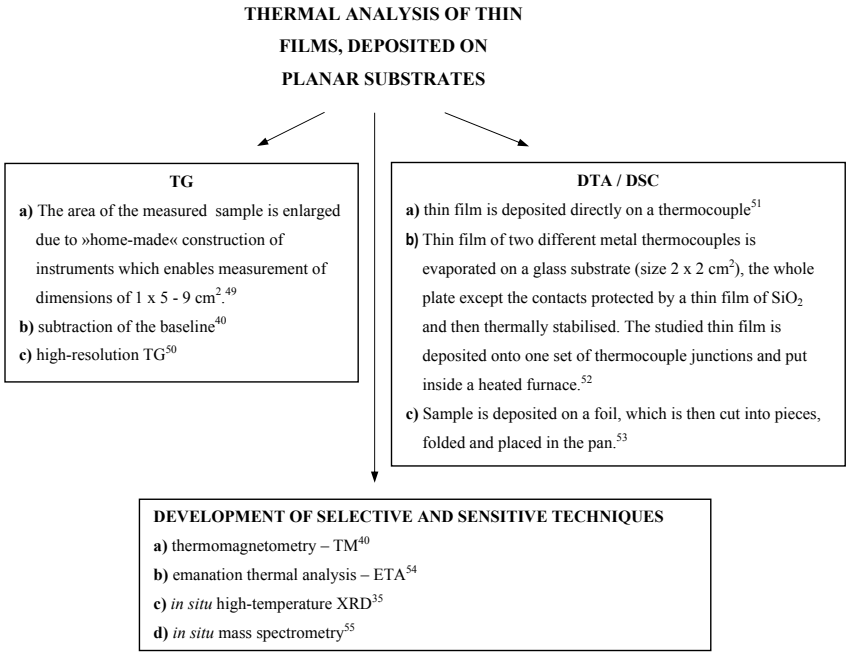

Figure 2. Basic strategies applied in thermal analysis of thin films, deposited on planar substrates.

combined with other measurements (XRD, EGA), useful information about structural changes and decomposition can be obtained.[57]

Our idea was to link the thermal analysis of thin films with the temperature-dependent electrochromic response of Ni oxide films. The first aim was a comparison between dynamic and isothermal TG curves of thin films and xerogels, prepared from $NiSO_4$ and $Ni(CH_3COO)_2$ precursors. On the basis of isothermal TG analysis, films with different ratios between the thermally undecomposed amorphous phase and nanosized Ni oxide were prepared. Their electrochromic properties were tested with additional spectroelectrochemical measurements, while changes in structure and morphology during thermal decomposition were followed using IR, TEM, AFM and EXAFS. As far as we know, this approach for optimising the electrochromic response was used for the first time in our laboratory.

4. Sol-gel prepared Ni oxide thin films from $NiSO_4$ precursor

Two different sols were prepared. For the first one, nickel sulfate heptahydrate (Kemika, p. a.) was taken as the precursor salt, whereas for the second sol nickel acetate tetrahydrate (Fluka, > 99%) was used. Both sols also contained acetic acid and a certain amount of lithium ions.[29,34] In Figure 3 dynamic TG curves under an air atmosphere of both thin films, deposited on a microscope cover glass, are presented. Thermal decomposition of the acetate groups occurs at 280 °C (onset temperature) for thin film of the $NiSO_4$ precursor and at 225 °C in the case of the $Ni(CH_3COO)_2$ precursor. For the corresponding xerogels, decomposition begins at 300 °C for the $NiSO_4$ precursor and 250 °C for the $Ni(CH_3COO)_2$ precursor.[29,34] During the combustion of acetate groups, the amorphous thin film or xerogel sample thermally decomposes and Ni oxide grains are formed inside the amorphous matrix. Thermal decomposition is finished at around 300 °C for the thin film of $Ni(CH_3COO)_2$ precursor and 330 °C for the thin film of $NiSO_4$ precursor.

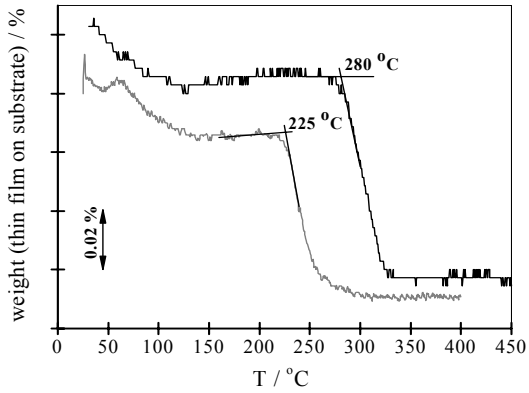

Figure 3. Comparison of dynamic TG curves of the two thin films. The black curve represents a thin film of $NiSO_4$ precursor and the grey curve a thin film of $Ni(CH_3COO)_2$ precursor.

In this section we will focus on thin films prepared from the $NiSO_4$ precursor. Samples with different stoichiometry between thermally undecomposed

amorphous phase and nanosized nickel oxide can be prepared on the basis of isothermal TG measurements (Figure 4). Since the thin film is deposited on a substrate, the exact weight loss on the ordinate scale is not known. To find out how much of the thin film sample decomposed at the isothermal temperature, the temperature after isothermal treatment was increased to 350 °C where decomposition was complete. The temperature profile during measurement is shown on the right hand ordinate scale. From the ratio of the isothermal weight loss after a defined time and the weight loss associated with decomposition of all acetate groups, the degree of thermal decomposition of acetate can be estimated.[29,34] When the thin films were exposed to 270 °C, the degree of thermal decomposition was 50% after 15 minutes, 80% after 30 minutes and 100% after 60 min. Thin films with different ratios between thermally undecomposed amorphous phase and nickel oxide can therefore be prepared by controlling the time of heat treatment at 270 °C. At 300 °C, the decomposition process is too fast (100% after 12 min) to control the stoichiometry. Only 30% decomposition of the amorphous xerogel was observed after 60 min at 270 °C; it was complete after 85 min at 300 °C.[34]

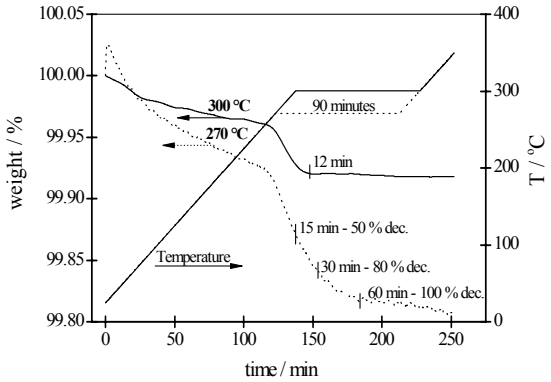

Figure 4. Isothermal TG curves of a thin film, prepared from $NiSO_4$ precursor, at 270 and 300 °C.

Evolution of IR spectra during heat treatment is shown in Figure 5. In a thermally untreated film the bands at 1565 and 1419 cm^{-1} correspond to acetate groups, mostly present as bridging ligands to nickel ions. Sulfate ions are monodentately, as well as bridge-bonded to nickel, and some of them are also adsorbed on colloidal particles[58] (the band at 1111 cm^{-1} belongs to a stretching vibration of the free sulfate ion). The intensities of acetate groups are lower after annealing the film at 270 °C for 15 min (c) and finally the vibrations disappear (e). In the spectra of films thermally treated at 270 °C for 15 min or more, the vibrations of the sulfate groups become characteristic of monodentate coordination. The Ni-O stretching band at 413 cm^{-1} becomes more and more intense (d, e). The band at ~ 1600 cm^{-1} is attributed to the bending vibration of water due to absorbed moisture.[58]

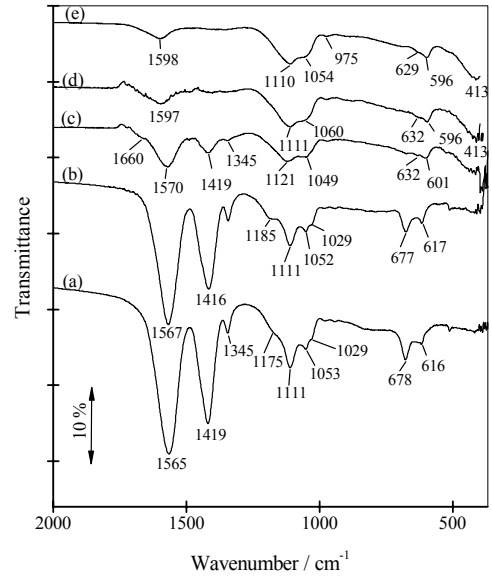

Figure 5. IR transmittance spectra of a thermally untreated film (a), film thermally treated for 15 min at 220 °C (b), for 15 min at 270 °C (c), for 30 min at 270 °C (d) and for 60 min at 270 °C (e).

Evolution of the surface during heat treatment is shown in Figure 6. The surfaces of the thin film samples (Figures B, C and D) are not smooth. The reason lies in the roughness of the substrate itself (Figure A), where the RMS roughness is 35 nm. After deposition of the sol, a nearly smooth surface is obtained (B). During heat treatment the film becomes thinner due to thermal decomposition and the surface more and more resembles that of the substrate (C, D). The RMS roughness is 10 nm in sample C and 18 nm in sample D. TEM micrographs (Figure 7) of a thin film thermally treated at 270 °C for 60 min show a uniform layer with a thickness of 35 nm (A). It consists of nano-crystals of cubic NiO with a size of 2 – 3 nm (B).

The monochromatic spectral transmittance changes (λ = 480 nm) detected during CV measurements of thin films, thermally treated to varying extents, are shown in Figure 8 A, B (1st cycle) and C, D (100th cycle). During the anodic scan the oxidation of Ni^{2+} to Ni^{3+} causes coloration of the film and consequently the transmittance decreases. In the reverse scan the reduction of Ni^{3+} leads to bleaching of the film. The maximal change in transmittance between the coloured and the bleached state in the 1st cycle was exhibited by a film heat treated for 15 min at 270 °C (43.1%). However, the decrease in the transmittance of the film in its bleached state by 1.9% at the end of the cycle shows that the reduction is not totally reversible. Films heat treated for 30 or 60 min at the same temperature

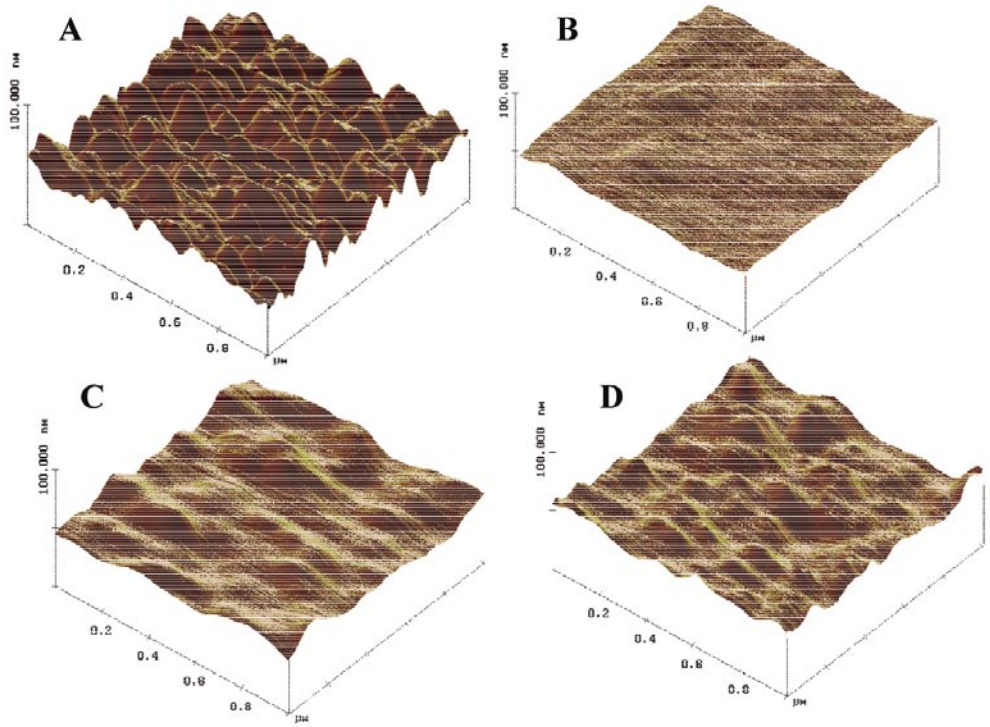

Figure 6. AFM images of a SnO_2/F surface – A; surface of a thermally untreated film, prepared from $NiSO_4$ precursor, after the dip-coating process – B; after thermal treatment at 270 °C for 15 min – C; and after thermal treatment at 270 °C for 60 min – D.

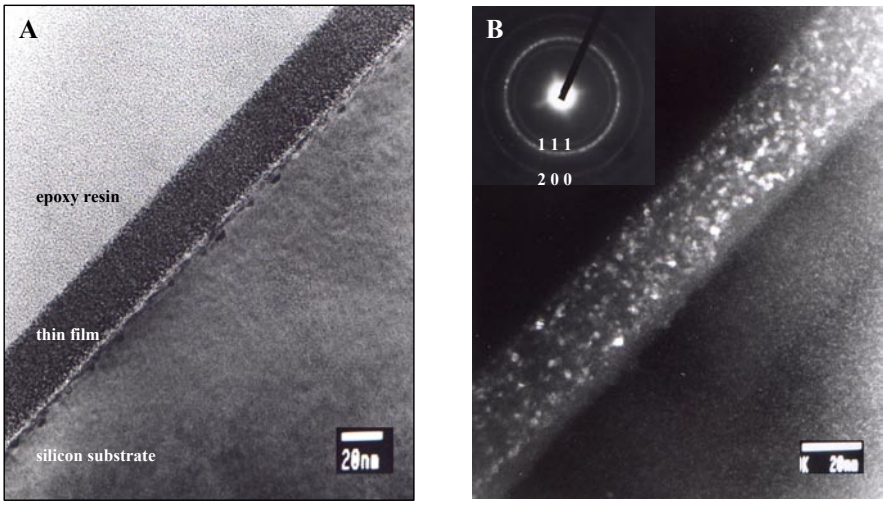

Figure 7. TEM micrograph (cross section - A) and dark field image and SAED pattern (inset, indexed as cubic NiO – B).

(270 °C) possess better reversibility (Figure 8A). CV measurements of these films (Figure 8B) are in accordance with the observed optical properties. The higher current densities indicate a greater number of active nickel ions for the least heat treated film (15 min at 270 °C), and the positions of the anodic and cathodic peaks reveal a more compact structure in those films exposed for 30 or 60 min to 270 °C. During the cycling process the number of active nickel ions increases: in the 100th cycle current densities are approximately 2.5 times higher than in the 1st cycle (Figure 8B, D). Approximately 50 cycles have to be performed to complete the activation period and reach the steady state. A film which was exposed for 60 min to 270 °C

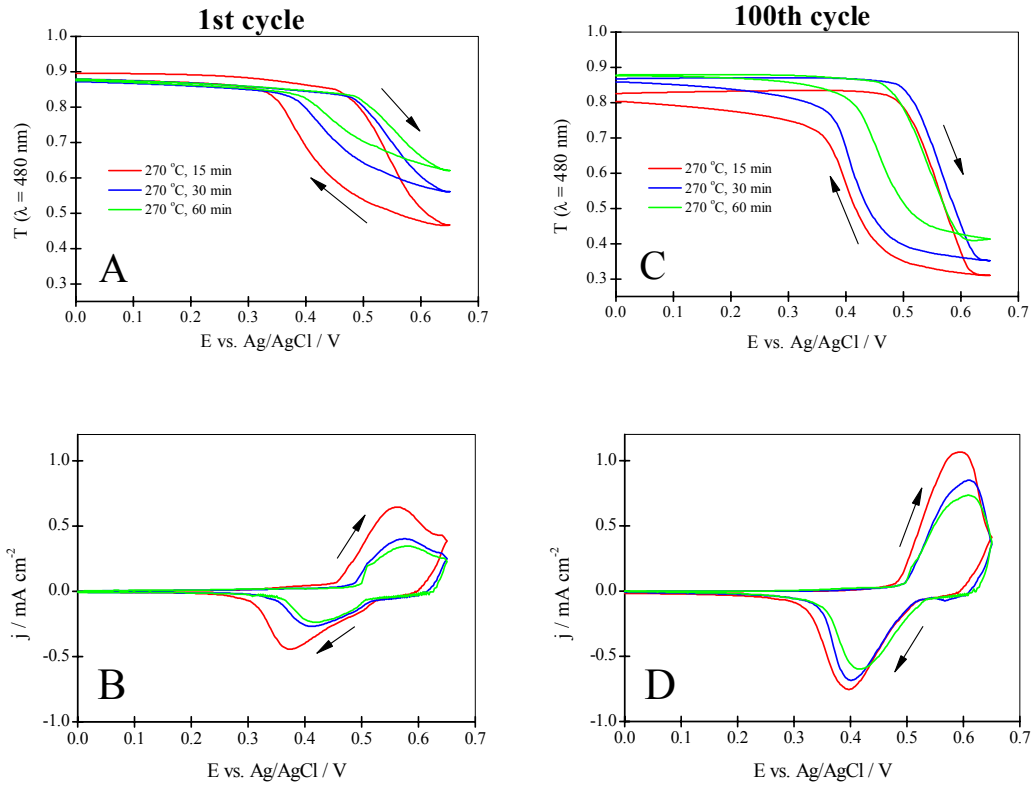

Figure 8. Monochromatic transmittance changes and cyclovoltammetric curves of different thermally treated Ni oxide thin films from a $NiSO_4$ precursor in 0.1 M LiOH – 1st cycle (A, B) and 100th cycle (C, D).

exhibited excellent reversibility in the 100th cycle. The transmittance change of 46.5% was smaller than for a thin film kept for 30 min at the same temperature (51.5%), but the latter did not bleach to the initial value in the 100th cycle (Figure 8C). The calculated *CE* for a film exposed at 270 °C for 60 min was – 41 cm^2 C^{-1} (λ = 480 nm) in the 100th cycle.

Reversibility in the bleaching process was also achieved for films thermally treated for 15 min at 400 °C (transmittance change in 100th cycle 40.6%) or 15 min at 500 °C (transmittance change 27.6%),[58] but of all films the highest coloration effect was exhibited by a thin film exposed for 60 min to 270 °C. During further heating (> 300 °C) the nano grains increased in size. The average size of the grains was 5 nm in a film treated for 15 min at 500 °C,[56] and sulfate ions remained monodentately bonded to nickel.[59] Assuming that electrochemical reaction takes place on the surface of the nano-grains, the coloration effect is less pronounced in films which consist of larger grains and have smaller specific surface values. Segregation of the grains could not be observed by TG measurements, since there is no weight loss. There was also no measurable change in heat flow signal on a DSC curve of a thin film between 300 and 400 °C.[34]

5. Sol-gel prepared Ni oxide thin films from $Ni(CH_3COO)_2$ precursor

On the basis of the results obtained for $NiSO_4$ precursor, we expected similar behaviour for thin films prepared from $Ni(CH_3COO)_2$ precursor; i.e. reversibility of the bleaching process after several cycles for a film where decomposition of the acetate groups is complete. However, the results obtained show that this film possesses quite different behaviour. Its isothermal

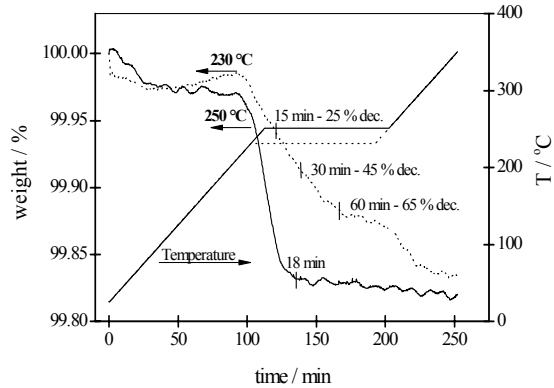

Figure 9. Isothermal TG curves of a thin film, prepared from $Ni(CH_3COO)_2$ precursor, at 230 and 250 °C.

TG curves at two different temperatures are shown in Figure 9. The degree of decomposition of the acetate groups is marked in the figure. For an amorphous xerogel only 8% decomposition was observed after 1h at 230 °C. At 250 °C, the decomposition of acetate groups was 90% after 60 min.[90]

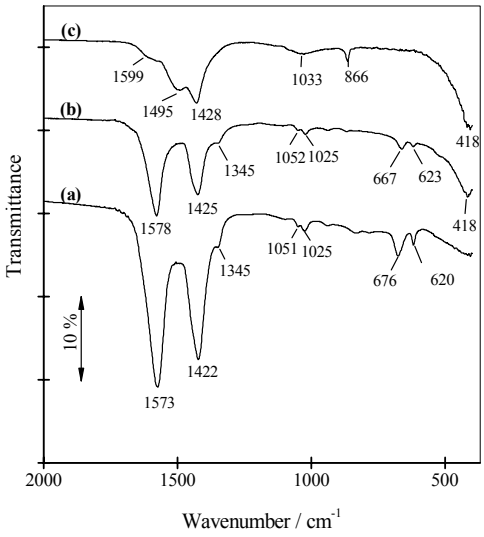

Figure 10. IR transmittance spectra of an as-deposited thin film prepared from $Ni(CH_3COO)_2$ precursor (a), and films thermally treated for 15 min at 230 °C (b) or 60 min at 230 °C (c).

In the IR spectrum of a thermally untreated film (Figure 10a) vibrations of bridge-bonded acetate groups can be identified. When the film is exposed to 230 °C for 15 min, these intensities are decreased (b). The new band appearing at 418 cm^{-1} indicates the formation of NiO. In a film which was exposed 60 min at 230 °C (c), vibrations of the carbonate groups, which originate from thermal decomposition of acetates, remain either free between the grains of nanosized Ni oxide or bidentately coordinated to nickel.[29]

In situ spectroelectrochemical measurements (Figure 11) show that for the acetate precursor optical reversibility is already achieved in a film thermally treated at 230 °C for 15 min (at least 75% of the film is still amorphous), but the size of the NiO grains already reaches 3 to 4 nm.[59] The monochromatic transmittance change is 40.6% in the 100th cycle (*CE* – 38 cm^2 C^{-1}). The slight difference in the response of the stabilized 100th cycle can therefore be attributed to the difference in the grain size, which was additionally confirmed by EXAFS measurements (Figure 12). Since the film from $Ni(CH_3COO)_2$ precursor with only 25% decomposition is electrochemically stable up to 100th cycle, we assume that the amorphous phase probably transforms into an electrochemically active phase during the cycling experiment. Films with a higher degree of heat treatment possess poorer electrochromic behaviour.

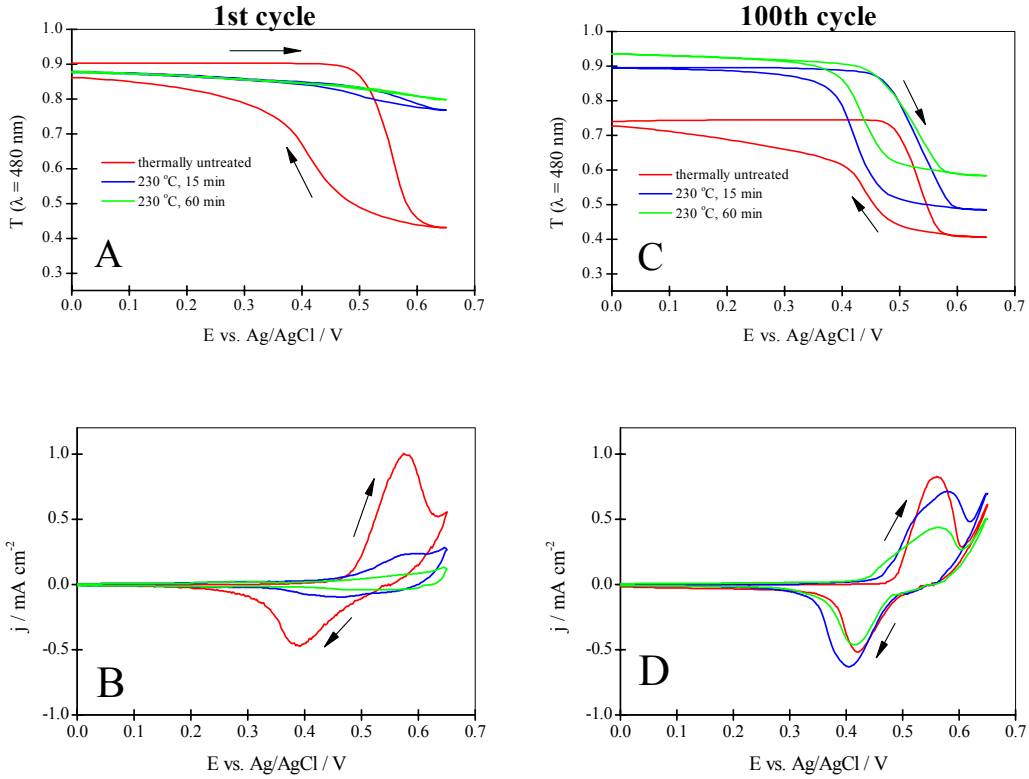

Figure 11. Monochromatic transmittance changes and cyclovoltammetric curves of different thermally treated Ni oxide thin films from a $Ni(CH_3COO)_2$ precursor in 0.1 M LiOH – 1st cycle (A, B) and 100th cycle (C, D).

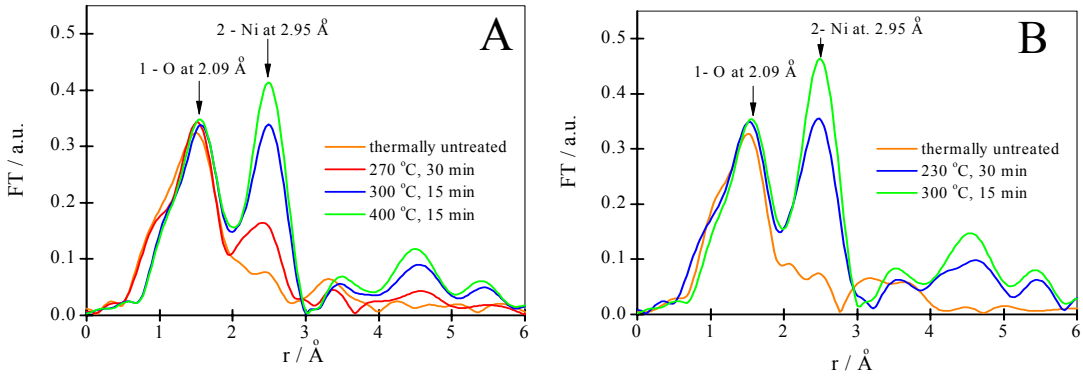

Figure 12. Fourier transforms of k weighted EXAFS spectra of thin films; k = 2.5 – 10.5 Å (A – $NiSO_4$ precursor; B – $Ni(CH_3COO)_2$ precursor). Th

The monochromatic transmittance change at λ = 480 nm in the 100th cycle is 28.8% for a film exposed for 30 min at 230 °C, and 34.9% for a film exposed for 60 min at 230 °C. The latter result is surprising, and from Figure 11A, C, it is evident that the initial transmittance of this film is higher after prolonged cycling. Some Ni^{3+} ions are probably present in the heat-treated film, which after the activation period are transformed to Ni^{2+} at the initial potential. The electrochromic performance of a film treated 15 min at 300 °C was poor. Its monochromatic transmittance change was 18.6% in the 100th cycle. The NiO grain size in this film ($Ni(CH_3COO)_2$ precursor, 100% decomposition) on average reached around 5 nm, but some of the grains were 7 nm.

Greater differences between optimized films from $NiSO_4$ precursor (60 min at 270 °C) and $Ni(CH_3COO)_2$ precursor (15 min at 230 °C) were observed at the beginning of cycling. The optical response of the film of $Ni(CH_3COO)_2$ precursor was very small (11%), whereas for the $NiSO_4$ precursor film it was 26%. The electrochemical mechanism at the beginning of the cycling process is most likely different in the two films.

From the EXAFS spectra (Figure 12) we can see that the first peak in the Fourier transforms is almost identical in all spectra, irrespective of the type of precursor and heat treatment applied. This agrees perfectly with a model with 6 equivalent oxygen neighbours. The observed Ni-O distance of 2.05 Å is characteristic of the NiO bunsenite structure. The second shell of neighbours reflects the ordering of the structure. Thermally untreated samples possess a loose structure with a small portion of higher components. In thermally treated samples, the second-neighbour peak can be modelled with 12 Ni atoms at 2.98 Å as in bunsenite. The results show that the thermal treatment increases order in the vicinity of Ni atoms. The films of $Ni(CH_3COO)_2$ precursor show a higher degree of crystallization than thin films from $NiSO_4$ precursor. This result is in accordance with TEM and spectroelectrochemical measurements. A comparison of k^3 weighted spectra of the measured data (film prepared from $NiSO_4$ precursor and heat-treated at 270 °C for 15 min) and its first two-shell model is given in Figure 13.

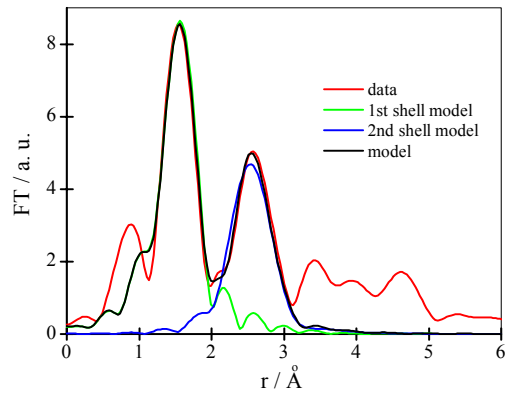

Figure 13. k^3 weighted spectrum of a film prepared from $NiSO_4$ precursor and heat-treated at 270 °C for 30 min (data), and its first two-shell model (model); k = 2.5 – 10.5 $Å^{-1}$.

5. Conclusion

The choice of precursor in sol-gel prepared Ni oxide thin films influences very much the properties of the final electrochromic material. We studied two precursors: $NiSO_4$ and $Ni(CH_3COO)_2$. The first difference between them was the temperature at which decomposition begins leading to formation of Ni oxide phase, which is approximately 50 degrees lower for the $Ni(CH_3COO)_2$ precursor. During thermal decomposition, carbonate ions bind bidentately to nickel or remain adsorbed in the structure in the case of $Ni(CH_3COO)_2$ precursor. When $NiSO_4$ precursor was used, sulfate ions remain monodentately bonded to nickel after thermal decomposition of acetates.

Larger Ni oxide grains are formed when $Ni(CH_3COO)_2$ was taken as precursor; at 100% decomposition of acetate groups they reached 5 nm on average, whereas in the case of $NiSO_4$ precursor the size of the grains was 2 - 3 nm. The grain size seems to be crucial for electrochromic response. Films prepared from $NiSO_4$ precursor have optimal response when decomposition of acetate is complete. For $Ni(CH_3COO)_2$ precursor films, optimal response is achieved when only 25% decomposition occurs and NiO grain size reaches 3 - 4 nm. The amorphous phase, present in the latter film, probably transforms into an electroactive phase during the activation period. Electrochromic properties in the steady state (100th cycle) for both optimised films are quite similar ($NiSO_4$ precursor, CE = – 41 cm^2 C^{-1}, transmittance change 46.5% at λ = 480 nm; $Ni(CH_3COO)_2$ precursor, CE = – 38 cm^2 C^{-1}, transmittance change 40.6% at λ = 480 nm). However, the initial electrochromic response of the two mentioned films is different and further investigations should be carried out in order to elucidate the differences in mechanisms during the activation period.

6. References

1. C. G. Granqvist: Handbook of Inorganic Electrochromic Materials, Elsevier Science, Amsterdam, **1995**, reprinted 2002.
2. S. K. Deb, *Philos. Mag.* **1973**, *27*, 801–822.
3. H. J. Byker, *Electrochim. Acta* **2001**, *46*, 2015–2022.
4. K. Bange, T. Gambke, *Adv. Mater.* **1990**, *2*, 10–16.
5. A. Azens, C. G. Granqvist, *J. Solid State Electrochem.* **2003**, *7*, 64–68.
6. C. M. Lampert, *Proc. SPIE* **2001**, *4458*, 95–97.
7. P. M. S. Monk, R. J. Mortimer, D. R. Rosseinsky: Electrochromism: Fundamentals and Applications, VCH, Weinheim, **1995**.
8. C. G. Granqvist, E. Avendano, A. Azens, *Thin Solid Films* **2003**, *442*, 201–211.
9. C. G. Granqvist: Chromogenic Materials for Transmittance Control of Large –Area Windows, in: Workshop on Materials Science and Physics of Non-Conventional Energy Sources, ICTP, Trieste, 11-29 September **1989**.
10. M. A. Aegerter: Sol-Gel Chromogenic Materials and Devices, in: Structure and Bonding, Vol. 85, Springer-Verlag, Berlin, **1996**, pp. 149–194.
11. S. Passerini, B. Scrosati, A. Gorenstein, *J. Electrochem. Soc.* **1990**, *137*, 3297–3300.
12. I. Hotovy, J. Huran, P. Siciliano, S. Capone, L. Spiess, V. Rehacek, *Sensors and Actuators* **2001**, *B78*, 126–132.
13. A. F. Wells: Structural Inorganic Chemistry, 5th Ed., Clarendon press, Oxford, **1984**, p. 538.
14. E. Antolini, *J. Mater. Sci.* **1992**, *27*, 3335–3340.
15. A. Agrawal, H. R. Habibi, R. K. Agrawal, J. P. Cronin, D. M. Roberts, R. S. Caron-Popowich, C. M. Lampert, *Thin Solid Films* **1992,** *221*, 239–253.
16. J. S. E. M. Svensson, C. G. Granqvist, *Appl. Phys. Lett.* **1986**, *49*, 1556–1568.
17. P. C. Yu, G. Nazri, C. M. Lampert, *Proc. SPIE* **1986**, *653*, 16–24.
18. J. Nagai, *Sol. Energy. Mater.* **1993**, *31*, 291–299.
19. I. Bouessay, A. Rougier, J.-M. Tarascon, *J. Electrochem. Soc.* **2004**, *151*, H145–H152.
20. E. Avendano, L. Berggren, G. A. Niklasson, C. G. Granqvist, A. Azens, *Thin Solid Films* **2006**, *496*, 30–36.
21. G. Boschloo, A. Hagfeldt, *J. Phys. Chem. B* **2001,** *105*, 3039–3044.
22. E. L. Miller, R. E. Rocheleau, *J. Electrochem. Soc.* **1997,** *144*, 1995–2003.
23. X. Chen, X. Hu, J. Feng, *Nanostruct. Mater.* **1995**, *6,* 309–312.
24. Z. Xuping, C. Guoping, *Thin Solid Films* **1997**, *298*, 53–56.
25. W. Estrada, A. M. Andersson, C. G. Granqvist, *J. Appl. Phys.* **1988**, *64*, 3678–3683.
26. I. Bouessay, A. Rougier, P. Poizot, J. Moscovici, A. Michalowicz, J.-M. Tarascon, *Electrochim. Acta* **2005**, *50*, 3737–3745.
27. P. K. Shen, H. T. Huang, A. C. C. Tseung, *J. Mater. Chem.* **1992**, *2*, 1141–1447.
28. M. Utriainen, M. Kröger-Laukkanen, L. Niinistö, *Mater. Sci. Eng.* **1998**, *B54*, 98–103.
29. R. Cerc Korošec, P. Bukovec, *Thermochim. Acta* **2004**, *410*, 65–71.
30. P. S. Patil, L.D. Kadam, *Appl. Surf. Sci.* **2002**, *199*, 211–221.
31. M. Chigane, M. Ishikawa, *J. Electrochem. Soc.* **1994**, *141*, 3439–3443.
32. M. C. A. Fantini, G. H. Bezerra, C. R. C. Carvalho, A. Gorenstein, *Proc. SPIE* **1991**, *1536*, 81–92.
33. A. Šurca, B. Orel, B. Pihlar, P. Bukovec, *J. Electroanal. Chem.* **1996,** *408,* 83–100.
34. R. Cerc Korošec, P. Bukovec, B. Pihlar, J. Padežnik Gomilšek, *Thermochim. Acta* **2003**, *402*, 57–67.
35. L. Niinistö, *J. Therm. Anal. Cal.* **1999**, *56,* 7–15.
36. P. K. Sharma, M. C. A. Fantini, A. Gorenstein, *Solid State Ionics* **1998,** *457*, 113–115.
37. A. Šurca, B. Orel, B. Pihlar, *J. Solid State Electrochem.* **1998,** *2*, 38–49.
38. P. A. Williams, A. C. Jones, J. F. Bikley, A. Steiner, H. O. Davies, T. J. Leedham, S. A. Impey, J. Garcia, S. Allen, A. Rougier, A. Blyr, *J. Mater. Chem.* **2001**, *11*, 2329–2334.
39. M. Leskelä, T. Leskelä, L. Niinistö, *J. Thermal. Anal. Cal.* **1993,** *4,* 1077–1088.
40. P. K. Gallagher, *J. Thermal. Anal.* **1992,** *38*, 17–26.
41. Y. Sawada, N. Mizutani, *Netsu Sokutei* **1989**, *16,* 185–194.
42. M. Leskelä, P. Eskelinen, M. Ritala, *Thermochim. Acta* **1993**, *214*, 19–26.

43. P. K. Gallagher, W. R. Sinclair, R. A. Fastnacht, J. P. Luongo, *Thermochim. Acta* **1974**, *8*, 141–148.
44. N. Tohge, A. Matsuda, T. Minami, *J. Am. Ceram. Soc.* **1987**, *70*, C13–C15.
45. M. Kumeda, H. Komatsu, T. Shimizu, *Thin Solid Films* **1985**, *129*, 227–230.
46. J. R. Bosnell, J. A. Savage, *J. Mater. Sci.* **1972**, *7*, 1235–1243.
47. D.S. Easton, E. H. Henninger, O. B. Cavin, C. C. Koch, *J. Mater. Sci.* **1983**, *18*, 2126–2134.
48. M. Kawarada, Y. Nishina, Japan. *J. Appl. Phys.* **1977**, *16*, 1531–1539.
49. S. Lieb, R. K. MacCrone, J. Theimer, E. W. Maby, *J. Mater. Res.* **1986**, *1*, 792–796.
50. P. S. Gill, S. R. Sauerbrunn, B. S. Crowe, *J. Thermal. Anal.* **1992**, *38*, 255–266.
51. F. Nava, G. Ottaviani, G. Riontino, *Mater. Lett.* **1985**, *3*, 311–313.
52. J. Przyłuski, J. Płocharski, W. Bujwan, *J. Thermal. Anal.* **1981**, *21*, 235–238.
53. S. Hackwood, G. Beni, P.K. Gallagher, *Solid State Ionics* **1981**, *2*, 297–299.
54. V. Balek, J. Fusek, O. Kriz, M. Leskelä, L. Niinistö, E. Nykänen, J. Rautanen, P. Soininen, *J. Mater. Res.* **1994**, *9*, 119–124.
55. E. Kinsbron, P. K. Gallagher, A. T. English, *Solid State Electron.* **1979**, *22*, 517–524.
56. P. K. Gallagher, *J. Therm. Anal.* **1997**, *49*, 33–44.
57. V. Balek, *Thermochim. Acta* **1978**, *22*, 1–156.
58. R. Cerc Korošec, P. Bukovec, B. Pihlar, A. Šurca Vuk. B. Orel, G. Dražič, *Solid State Ionics* **2003**, *165*, 191–200.
59. R. Cerc Korošec, Ph.D. Thesis (in Slovene), University of Ljubljana, Ljubljana, Slovenia, **2001**, p. 135, 136.

Povzetek

Elektrokromni materiali pri določenem potencialu spremenijo svoje optične lastnosti v vidnem delu spektra. Sprememba je reverzibilna in materialu se povrnejo prvotne lastnosti v nasprotnem električnem polju. Elektrokromne lastnosti materialov uporabljamo v elektrokromnih sklopih, kjer v večplastnemu, bateriji podobnemu sestavu s pomočjo električne napetosti reguliramo količino sončnega sevanja skozi okno in ga zato imenujemo pametno okno. V prvem delu članka so jedrnato predstavljene teoretične osnove elektrokromizma ter princip delovanja pametnega okna. Nikljev oksid so v zadnjem desetletju veliko preučevali kot hranilnik ionov v elektrokromnih sklopih, zato so v nadaljevanju podane nekatere njegove lastnosti. Termična obdelava tankih plasti nikljevega oksida v veliki meri določa elektrokromni odziv (stopnjo obarvanja, reverzibilnost med preklapljanem napetosti) teh plasti. Kadar tanke plasti pripravljamo s kemijskimi postopki nanašanja, lahko iz rezultatov termične analize dobimo koristne informacije o primerni temperaturi in času toplotne obdelave. Termična analiza tankih plasti, nanesenih na podlago, ne spada med klasične analizne tehnike, zato so v članku zbrani osnovni pristopi k tem meritvam. Po teoretičnem uvodu je v članku prestavljena metoda optimizacije elektrokromnega odziva nikelj-oksidnih tankih plasti, pripravljenih po sol-gel postopku. Elektrokromne lastnosti termično različno obdelanih tankih plasti smo testirali s pomočjo spektroelektrokemijskih meritev, z IR, TEM, AFM in EXAFS pa smo spremljali strukturne in morfološke spremembe med segrevanjem.